



HAL
open science

UAV detection with K band embedded FMCW radar

Israël Hinostroza, Thierry Letertre, Valentin Mazieres

► **To cite this version:**

Israël Hinostroza, Thierry Letertre, Valentin Mazieres. UAV detection with K band embedded FMCW radar. 2017 Mediterranean Microwave Conference (MMS), Nov 2017, Marseille, France. pp.1-4, 10.1109/MMS.2017.8497143 . hal-02414042

HAL Id: hal-02414042

<https://centralesupelec.hal.science/hal-02414042>

Submitted on 17 Jun 2021

HAL is a multi-disciplinary open access archive for the deposit and dissemination of scientific research documents, whether they are published or not. The documents may come from teaching and research institutions in France or abroad, or from public or private research centers.

L'archive ouverte pluridisciplinaire **HAL**, est destinée au dépôt et à la diffusion de documents scientifiques de niveau recherche, publiés ou non, émanant des établissements d'enseignement et de recherche français ou étrangers, des laboratoires publics ou privés.

UAV detection with K band embedded FMCW radar

Israel Hinostraza*, Thierry Letertre* and Valentin Mazières

SONDRA
CENTRALESUPELEC
Gif-sur-Yvette, France

*{First_name.Last_name}@centralesupelec.fr

Abstract—Electromagnetic simulations of a propeller, motor and arm of a commercially available UAV are presented. The goal was to identify the incidence angles of the wave where there is a strong variation of the radar cross section of the structure due to the position of the propeller, which will help in the Doppler analysis. Additionally measurements of the UAV were performed using a commercially available 24-GHz FMCW radar. Two scenarios were considered: hovering and vertical movement. In both cases the Doppler signature is characteristic.

Keywords—octocopter; K band; FMCW radar; propeller, embedded

I. INTRODUCTION

As the cost of small UAVs has become affordable, their number has been increasing. Some of these UAVs can carry up to 2.5 Kg with a diameter of 75 cm and maximum speed flight of 15 m/s. Due to their small size and low speed their radar detection and identification can be challenging. Analysis of the RCS of small propellers has been done from 1 – 10 GHz [1], [2] and Doppler signatures of small multi-rotors (quadrotor, hexarotor, octorotor) have been investigated in the same bandwidth [1], [3].

The goal of this study is to investigate the feasibility of the detection of a UAV using a small portable radar that can be embedded in another UAV. We present some RCS simulations of a propeller, motor and one arm of a UAV (OktoXL from Mikrokopter) at 24 GHz. Detection of a UAV (range-time and range-doppler diagrams), with a commercially available FMCW radar at 24 GHz (from IMST), while hovering and during vertical movement are also presented for different resolutions.

II. PROPELLER RCS SIMULATIONS

Micro Doppler analysis of small UAVs can help in their classification and discrimination from other objects with similar sizes [micro doppler UAV1, and microdopplerUAV2]. Strong changes in the radar cross section (RCS) of the moving parts (propeller) of the UAV help in the micro-Doppler analysis. The RCS (HH) of a propeller (12", ~ 30.5 cm), motor and one arm (40x1x1 cm) of the Okto XL was obtained through simulation in FEKO (see Fig. 1) for a frequency of 24 GHz. The structure was modelled as perfect electric conductor. Fig. 1 shows the propeller at position 0deg (along x axis) and the different planes of simulation. Fig. 2 and 3 show the simulation results for the planes XOZ and YOZ, respectively, for 2 perpendicular positions of the propeller: 0deg (propeller along x axis) and 90deg (propeller along y axis). From Fig. 2, it can be seen that changes in RCS due to the propeller position

are negligible for most of the angles of incidence in the plane XOZ. In fact, the RCS is dominated by the arm of the UAV, especially for incidences at $\theta = 90$ deg and 270deg (lateral incidence). At $\theta = \pm 30$ deg and ± 160 deg the propeller position has a larger impact on the RCS of the structure.

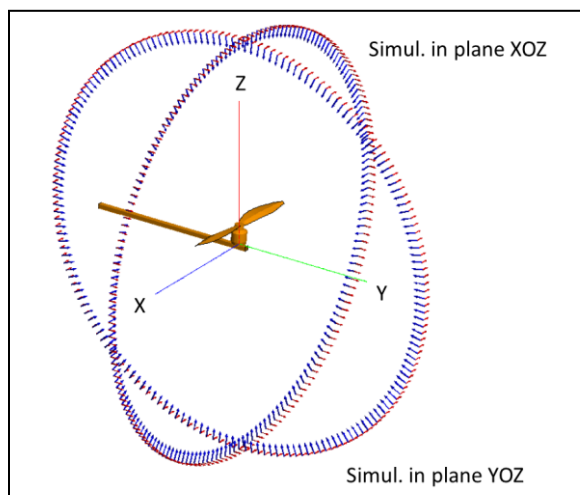


Fig. 1. Configuration of motor, arm and propeller (12") at position 0deg of Okto XL.

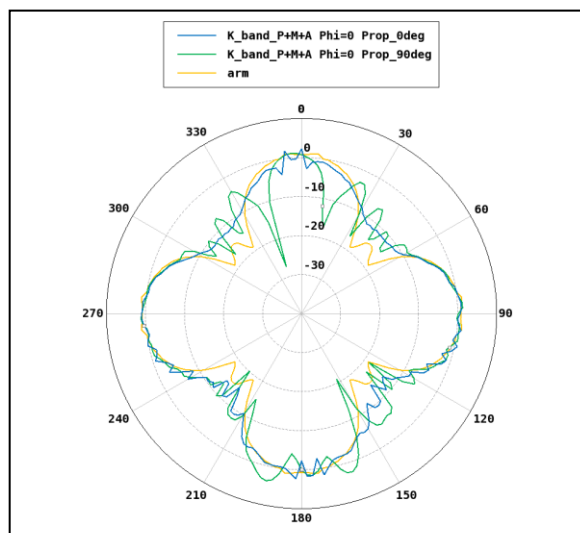


Fig. 2. RCS (dBsm) of single OktoXL arm (yellow) and whole structure of Fig. 1 for the plane XOZ for 2 positions of the propeller: 0deg (blue) and 90deg (green).

From Fig. 3, it can be seen that maximum change in RCS (minimum of 10 dB) due to the position of the propeller is at

around $\theta = \pm 30\text{deg}$ and $\pm 150\text{deg}$. These angles, will facilitate the detection of the UAV through the analysis of the Doppler shift caused by the rotation of the propellers for the case of HH polarization. But the RCS (due to the arm) is 10 dB lower than the RCS (due to the arm) at $\theta = 0\text{deg}$ and 180deg (incidence from above and below, respectively). Hence, vertical movement (along z axis), especially those including

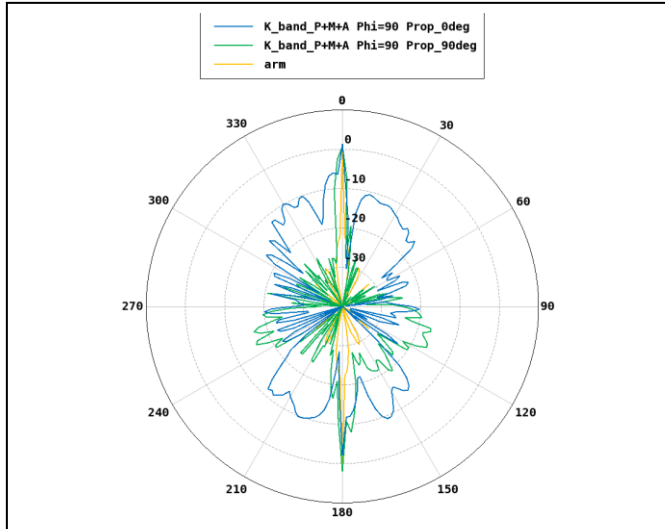


Fig. 3. RCS (dBsm) of single OktoXL arm (yellow) and whole structure of Fig.1 for the plane YOZ for 2 positions of the propeller: 0deg (blue) and 90deg (green).

TABLE I. PARAMETERS OF FMCW RADAR

Symbol	Description	Value
F_R	Sweep repetition frequency	16.7 Hz
U_T	Up-ramp time	1ms
n_{ramp}	Number of samplings per ramp	1024
BW	Bandwidth of ramp	250 MHz and 2 GHz
P	Emitted power as EIRP	20 dBm
P_{Tot}	Max. total power consumption	5 W
W	Weight	300 g

TABLE II. CHARACTERISTICS OF UAV OKTOXL

Description	Value
Max. diameter motor to motor	73 cm
Max. weight (incl. payload)	5 Kg
Rotation of propellers	2000 – 5000 rev/min
Total length of propellers	12", ~ 30.5 cm
Motors MK3638	8
Max. horizontal speed	18 m/s
Max. vertical speed	8 m/s
Max. power consumption	800 W

III. FMCW RADAR MEASUREMENTS

The radar used is the 24-GHz-FMCW from IMST GmbH. The configurations of the radar for this study are presented in Table I. Measurements were done for the HH polarization. The UAV used was the OktoXL, shown in Fig. 4, upper-left corner. Main characteristics of the UAV are presented in Table II. The UAV uses 8 motors with carbon fiber propellers of 12" length (~ 30.5 cm) and rotation between 2000 to 5000 rev/min (~ 34 to 84 Hz). 4 motors rotate in opposite direction to the 4 others to compensate the torque. Fig. 4 also shows the position of the radar and the area of movement of the UAV.

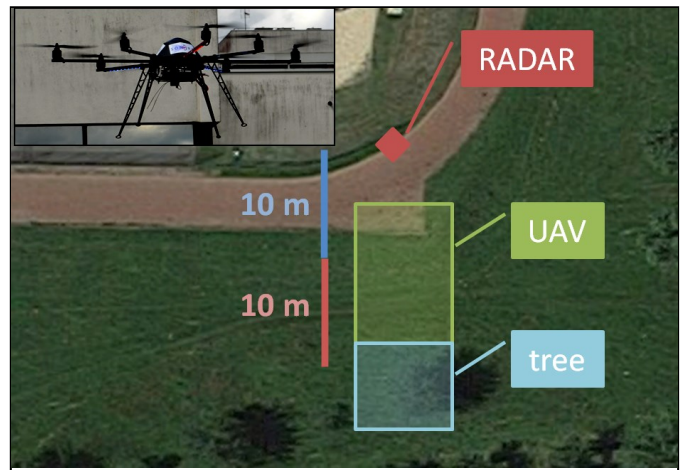


Fig. 4. OktoXL (upper-left corner), position of the radar (red rhombus), area of movement of the UAV (green semi-transparent rectangle) and tree (light blue). Place: running track at CentraleSupélec, Gif-sur-Yvette.

From the half-length of the propeller and the minimum rotation of the propellers (2000 rev/min to compensate the UAV's weight), the velocity at the tip of the propellers is at least 32 m/s. For a wave of 24 GHz, the frequency Doppler shift is then at least 5.12 KHz, much higher than F_R . Hence, aliasing of the Doppler frequency will occur as in [3]. From previous section, vertical movement of the UAV will facilitate the observation of the strong Doppler shift caused by the rotation of the propellers.

Fig. 5 and Fig. 6 show the range-time and range-doppler diagrams for different types of flights (hovering and slow vertical movement) of the UAV and different BW (radar bandwidth, 250 MHz or 2 GHz). Diagrams of range-time are presented alongside their respective range-doppler diagrams. The size of each measurement is 1024x81. Only the area of interest is shown (1 – 19 m) in the figures.

A. Measurements with 250 MHz bandwidth

In Fig. 5 (a) and (b) we can see the UAV hovering at 6.6 m from the radar. As explained before, there is aliasing in Doppler frequency due to the low sweep repetition frequency of the radar. Additionally, while hovering the UAV is still moving. This is observed in the slightly higher levels of the spectrum in the positive Doppler frequencies in Fig. 5 (b). In Fig. 5 (c) and (d) we can see the UAV during a slow vertical movement. In general, the scattered signal levels (Fig. 5-c) are smaller than in the previous case (hovering, Fig. 5-a) since the UAV is farther from the radar. From the range-doppler

diagram, Fig. 5 (d), we can see that the UAV was getting farther from the radar (stronger negative Doppler frequencies). In Fig. 5 (c) we also observe some echoes at 5.4 m and 7.2 m. Their Doppler signatures indicate that they correspond to objects that are not moving. These are the borders of the running track (see Fig. 4).

B. Measurements with 2 GHz bandwidth

In Fig. 6 (a) and (b) we can see the UAV hovering at 10 m from the radar. In Fig. 6 (c) and (d) we can see the UAV during a slow vertical movement. Aliasing in Doppler frequency is again present as observed in Fig. 6 (b). As in the previous subsection, the vertical movement of the UAV was done at a farther distance than the hovering case. This explains the smaller signal levels for the case of vertical movement (Fig. 6-c) with respect to the hovering case (Fig. 6-d). In the range-doppler diagram, Fig. 6 (d), at the area of movement (9.5 – 11 m), the image is smeared due to the movement of the UAV. Comparing with the previous section, the scattered signals of the borders of the running track are less important than the one from the ground close to the radar (Fig. 6-a and 6-c). The range-doppler diagram confirms that these signals correspond to non-moving objects. Additionally, signatures of the UAV in the range-time of Fig. 6 (a) and range-doppler diagrams of Fig. 6 (b) and (d) have a width of about 80 cm which corresponds well to the diameter D (73 cm, see Table II) of the UAV.

C. Doppler frequency signatures of UAV and tree

Previously we have seen that non-moving objects get easily differentiated from the UAV comparing their Doppler spectra. In Fig. 4 we can observe a tree not too far from the UAV. Its horizontal canopy diameter is about 5 m (between 19 – 24 m from the radar). In Fig. 7 and Fig. 8 we can compare the Doppler spectra of the hovering UAV and the tree for different radar BWs, 250 MHz and 2 GHz, respectively.

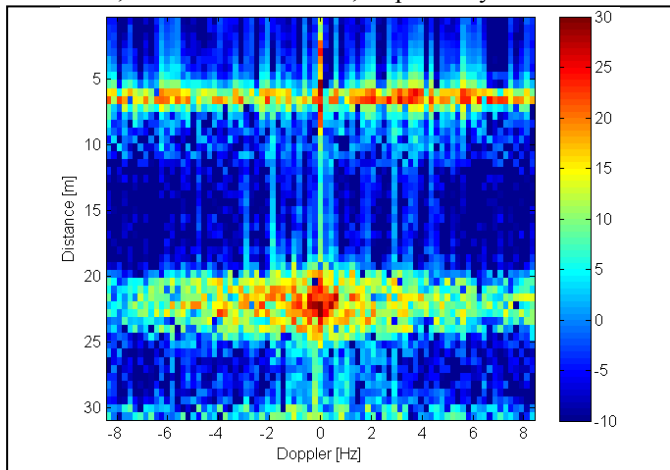


Fig. 7. Range-doppler diagram of hovering UAV at 6.6 m and trees (see Fig. 4), BW=250 MHz. Extension of Fig. 5 (a).

From Fig. 7 we can easily identify the non-moving part of the tree, the trunk, revealed by the strong levels of the Doppler spectrum around 0 Hz at 22 m. Due to the wind the branches of the tree were moving which is revealed in the non-zero frequencies for ranges between 19 – 25 m. In Fig. 8 the Doppler spectrum of the tree is much less clear. The trunk is not visible but non-zero Doppler frequencies indicate that there

is movement at about the tree's location. This difference can be related to the different resolutions obtained in the images. In Fig. 7 the range resolution is 0.6 m and in Fig. 8 it is 0.075 m. Hence there is much more energy in one pixel of Fig. 7 than in one of Fig. 8.

Then, there is a clear difference of the Doppler signature of the UAV and the one of a tree moved by the wind for both resolutions.

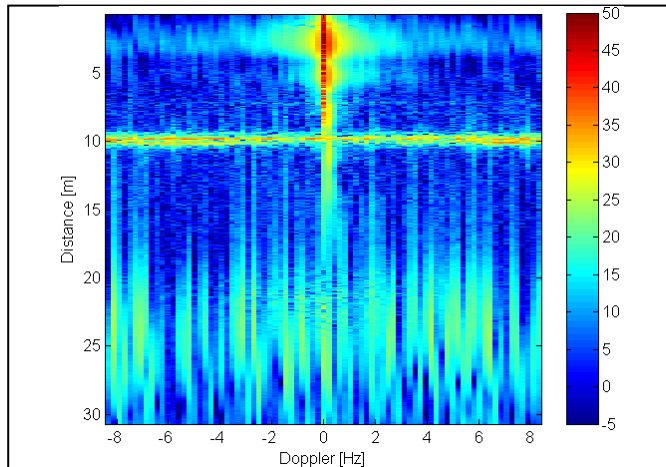


Fig. 8. Range-doppler diagram of hovering UAV at 10 m and trees (see Fig. 4), BW=2 GHz. Extension of Fig. 6 (a).

CONCLUSIONS

Simulations done in FEKO have shown that the changes in RCS of a PEC structure of propeller, motor and arm are large at certain angles ($\theta = \pm 30\text{deg}$ and $\pm 150\text{deg}$, geometrical reference Fig. 1) are large for HH polarization. Due to the high speed of the propellers and the low sweep repetition frequency of the FMCW radar, aliasing in the Doppler spectrum is always present in the UAV signature. The rich frequency content in the Doppler spectrum may be used to identify the presence of hovering UAVs close to bigger objects, as a tree, which have a much different frequency signature.

REFERENCES

- [1] M. Ritchie, F. Fioranelli, H. Griffiths and B. Torvik, "Micro-drone RCS analysis", 2015 IEEE Radar Conference, Johannesburg, South Africa, 2015.
- [2] Z. J. Meng, M. Y. Lu and Z. Wu, "Experimental analysis of electromagnetic scattering by rotating blades", 4th European Conference on Antennas and Propagation (EuCAP), Barcelona, Spain, 2010.
- [3] J. J. M de Witt, R. I. A. Harmanny and G. Premel-Cabic, "Micro-Doppler Analysis of Small UAVs", 9th European Radar Conference, Amsterdam, Netherlands, 2012.

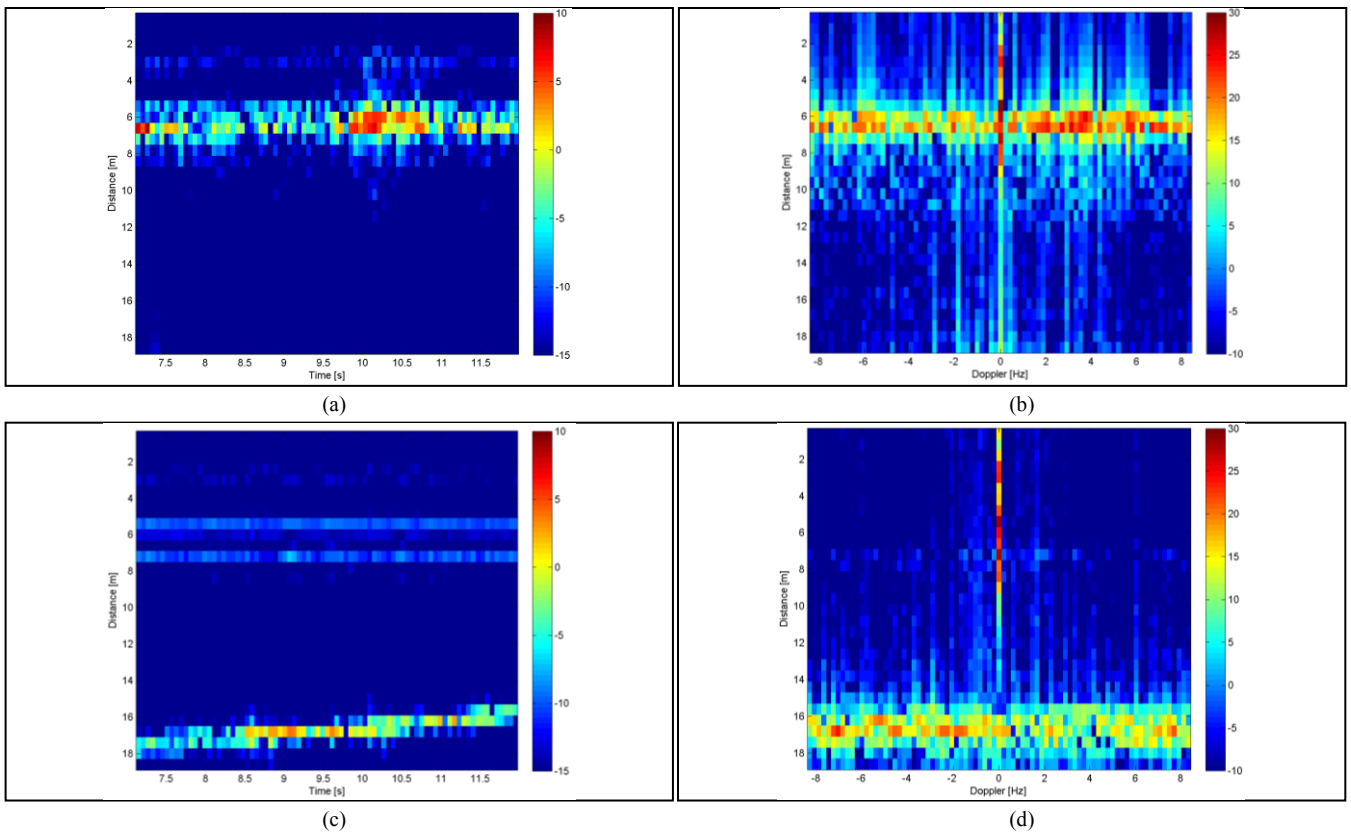


Fig. 5. UAV during hovering: range-time (a) and range-doppler (b). UAV during slow vertical movement: range-time (c) and range-doppler (d). All cases for bandwidth 250 MHz.

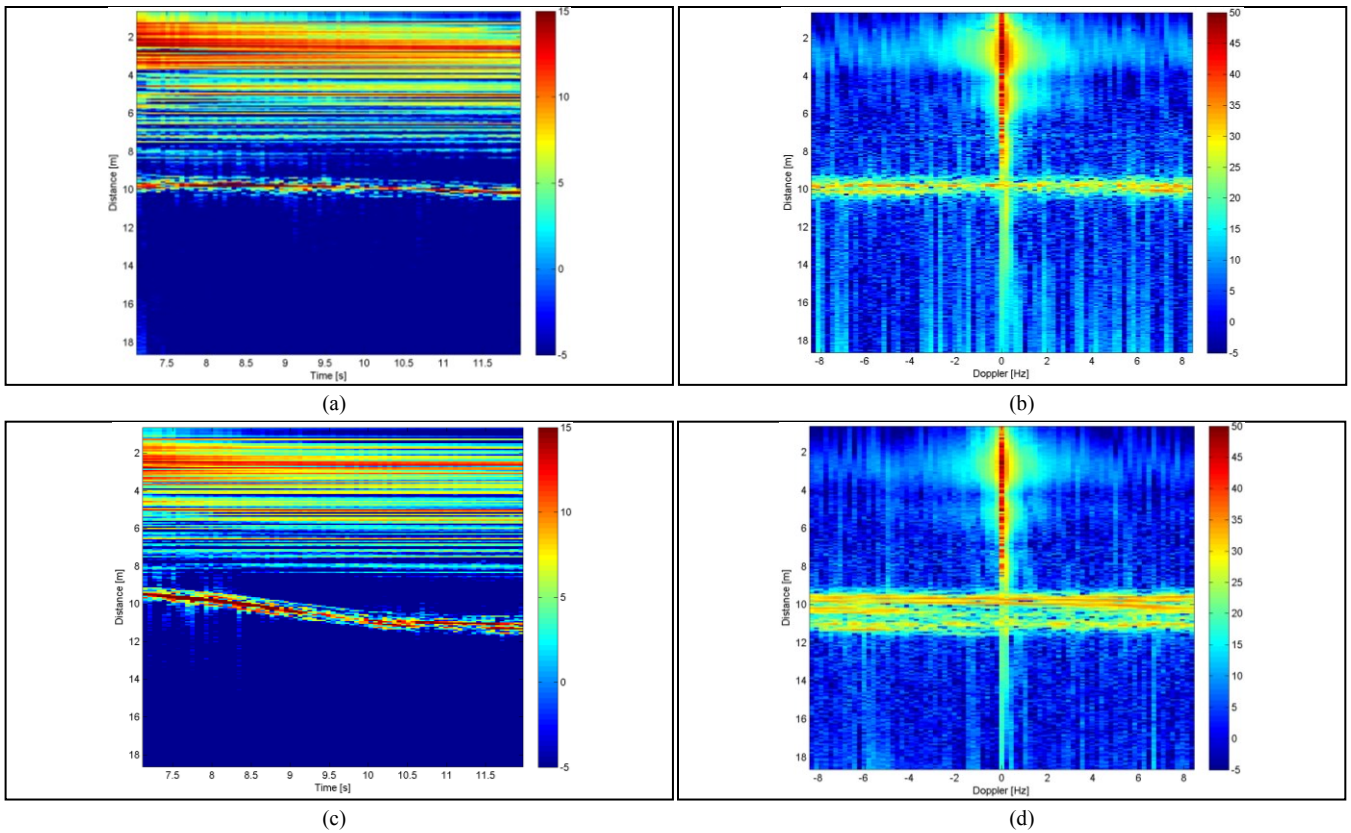


Fig. 6. UAV during hovering: range-time (a) and range-doppler (b). UAV during slow vertical movement: range-time (c) and range-doppler (d). All cases for bandwidth 2 GHz.